

Selective Transport of Monoamine Neurotransmitters by Human Plasma Membrane Monoamine Transporter and Organic Cation Transporter 3^[S]

Haichuan Duan and Joanne Wang

Department of Pharmaceutics, University of Washington, Seattle, Washington

Received May 7, 2010; accepted September 20, 2010

ABSTRACT

The plasma membrane monoamine transporter (PMAT) and organic cation transporter 3 (OCT3) are the two most prominent low-affinity, high-capacity (i.e., uptake₂) transporters for endogenous biogenic amines. Using the Flip-in system, we expressed human PMAT (hPMAT) and human OCT3 (hOCT3) at similar levels in human embryonic kidney 293 cells. Parallel and detailed kinetics analysis revealed distinct and seemingly complementary patterns for the two transporters in transporting monoamine neurotransmitters. hPMAT is highly selective toward serotonin (5-HT) and dopamine, with the rank order of transport efficiency (V_{\max}/K_m) being: dopamine, 5-HT \gg histamine, norepinephrine, epinephrine. The substrate preference of hPMAT toward these amines is substantially driven by large (up to 15-fold) distinctions in its apparent binding affinities (K_m). In contrast, hOCT3 is less selective than hPMAT toward the

monoamines, and the V_{\max}/K_m rank order for hOCT3 is: histamine > norepinephrine, epinephrine > dopamine > 5-HT. It is noteworthy that hOCT3 demonstrated comparable (≤ 2 -fold difference) K_m toward all amines, and distinctions in V_{\max} played an important role in determining its differential transport efficiency toward the monoamines. Real-time reverse transcription-polymerase chain reaction revealed that hPMAT is expressed at much higher levels than hOCT3 in most human brain areas, whereas hOCT3 is selectively and highly expressed in adrenal gland and skeletal muscle. Our results suggest that hOCT3 represents a major uptake₂ transporter for histamine, epinephrine, and norepinephrine. hPMAT, on the other hand, is a major uptake₂ transporter for 5-HT and dopamine and may play a more important role in transporting these two neurotransmitters in the central nervous system.

Introduction

The monoamines, including the catecholamines (dopamine, epinephrine, norepinephrine), serotonin (5-HT), and histamine, are a group of important neurotransmitters and neurohormones. Monoamines regulate a wide array of physiological, behavioral, cognitive, and endocrine functions in central and peripheral nervous systems (Carlsson, 1987; Greengard, 2001). The actions of released monoamine neurotransmitters are terminated by plasma membrane transporters that actively remove the transmitters from the extra-

cellular space. Two distinct transport systems, named uptake₁ and uptake₂, are responsible for the clearance of monoamines (Gründemann et al., 1998; Eisenhofer, 2001). Uptake₁ consists of Na⁺- and Cl⁻-dependent, high-affinity transporters in the solute carrier 6 family and includes the 5-HT transporter (SERT; SLC6A4), the dopamine transporter (DAT; SLC6A3), and the norepinephrine transporter (NET; SLC6A2) (Blakely et al., 1994; Torres et al., 2003). Predominantly expressed on the nerve endings of monoaminergic neurons, uptake₁ transporters are the major mechanism for clearing released transmitters from the synaptic cleft. They are also the targets for numerous clinically significant agents such as antidepressants and drugs of abuse (Amara and Kuhar, 1993; Torres et al., 2003).

The uptake₂ was originally characterized as a Na⁺- and Cl⁻-independent, low-affinity, high-capacity transport system in peripheral tissues such as heart and smooth muscle

This work was supported by the National Institutes of Health National Institute of General Medicine Sciences [Grants GM066233, GM066233-07S1]. Article, publication date, and citation information can be found at <http://jpet.aspetjournals.org>. doi:10.1124/jpet.110.170142.

[S] The online version of this article (available at <http://jpet.aspetjournals.org>) contains supplemental material.

ABBREVIATIONS: 5-HT, serotonin; SERT, 5-HT transporter; PMAT, plasma membrane monoamine transporter; hPMAT, human PMAT; CNS, central nervous system; SLC, solute carrier family; D22, decynium-22 (1,1'-diethyl-2,2'-cyanine); DAT, dopamine transporter; GUSB, β -glucuronidase; MPP⁺, 1-methyl-4-phenylpyridinium; NET, norepinephrine transporter; OCT, organic cation transporter; hOCT, human OCT; TEA, tetraethylammonium; HEK, human embryonic kidney; RT-PCR, reverse transcription-polymerase chain reaction; FBS, fetal bovine serum; DPBS, Dulbecco's phosphate-buffered saline; GBR12909, 1-[2-[bis(4-fluorophenyl)methoxy]ethyl]-4-(3-phenylpropyl)piperazine; FRT, flippase recognition target.

cells (Iversen, 1971; Bönisch et al., 1985; Eisenhofer, 2001). Historically, uptake₂ has been associated with monoamine metabolism and was proposed to play a backup role in monoamine uptake (Gründemann et al., 1998; Eisenhofer, 2001). However, emerging data suggest that these transporters may be actively involved in various monoamine signaling pathways and may represent promising targets for neuropsychiatric and neurodegenerative disorders (Schildkraut and Mooney, 2004; Zhou et al., 2007; Cui et al., 2009; Daws, 2009).

The molecular identity of uptake₂ was unclear until recently. Molecular cloning work, including that from our laboratory, suggests that uptake₂ consists of multiple organic cation transporters with broad substrate selectivity (Gründemann et al., 1998; Wu et al., 2000; Engel et al., 2004; Daws, 2009). In particular, the organic cation transporter 3 (OCT3; also termed extraneuronal monoamine transporter) and the plasma membrane monoamine transporter (PMAT) are the two most prominent uptake₂ transporters for endogenous monoamines (Gründemann et al., 1998; Wu et al., 2000; Engel et al., 2004; Daws, 2009). OCT3 (SLC22A3) and PMAT (SLC29A4) both transport a broad range of organic cations, including monoamine neurotransmitters and the prototypical organic cations 1-methyl-4-phenylpyridinium (MPP⁺) and tetraethylammonium (TEA) (Gründemann et al., 1998; Kekuda et al., 1998; Engel et al., 2004; Engel and Wang, 2005). OCT3- and PMAT-mediated monoamine transport show classic uptake₂ characteristics, such as Na⁺ and Cl⁻ independency and low substrate affinity but high transport capacity (Wu et al., 1998; Engel et al., 2004). Both transporters are highly sensitive to inhibition by the isocyanine compound, decynium 22 (D22) (Hayer-Zillgen et al., 2002; Engel et al., 2004). However, OCT3 is highly sensitive to corticosterone, whereas PMAT is not (Hayer-Zillgen et al., 2002; Engel et al., 2004). OCT3 and PMAT have been reported to be expressed in the brain and a number of peripheral tissues (Slitt et al., 2002; Engel et al., 2004). In rodent brains, *in situ* hybridization and immunolocalization work suggested that Oct3 and Pmat are expressed in neuronal cells in many brain regions (Amphoux et al., 2006; Dahlin et al., 2007; Gasser et al., 2009). Oct3 is also reported to be expressed in astroglial cells (Cui et al., 2009; Gasser et al., 2009).

The large overlaps in substrate specificity and tissue distribution of OCT3 and PMAT raise important questions regarding their specific contribution to monoamine clearance *in vivo*. Although both transporters have been characterized in several studies (Gründemann et al., 1998, 1999; Wu et al., 2000; Hayer-Zillgen et al., 2002; Engel et al., 2004; Engel and Wang, 2005), comprehensive and parallel analyses have not been performed to compare their substrate selectivity and transport kinetics for endogenous monoamines. Furthermore, although the expression patterns of Oct3 and Pmat have been studied in rat and mouse brains (Amphoux et al., 2006; Dahlin et al., 2007; Vialou et al., 2007), little is known regarding their relative expression levels in various human brain areas. The current study is designed to compare the intrinsic transport efficiencies of human PMAT and human OCT3 for endogenous monoamines. Using the Flp-in system, we stably expressed hPMAT and hOCT3 at comparable levels in HEK293 cells and compared their transport kinetics toward monoamines. We then determined and compared the expression levels of the two transporters in various human

brain regions and tissues. Finally, we evaluated the contribution of each transporter to 5-HT clearance through mouse brain synaptosome uptake studies.

Materials and Methods

Materials. [³H]MPP⁺ (85 Ci/mmol) was purchased from American Radiolabeled Chemicals, Inc. (St. Louis, MO). [³H]5-HT (28 Ci/mmol), [³H]dopamine (51.3 Ci/mmol), [³H]epinephrine (77 Ci/mmol), [³H]norepinephrine (5.3 Ci/mmol), [³H]histamine (14.2 Ci/mmol), and [¹⁴C]tetraethylammonium (3.5 mCi/mmol) were purchased from PerkinElmer Life and Analytical Sciences (Waltham, MA). Nonradiolabeled chemicals were purchased from Sigma-Aldrich (St. Louis, MO). Cell culture media and reagents were from Invitrogen (Carlsbad, CA). Cell culture plasticware was from BD Biosciences (San Jose, CA) or Corning Life Sciences (Lowell, MA).

Cell Culture. Flp-in HEK293 cells were purchased from Invitrogen and maintained in Dulbecco's modified Eagle's medium (high glucose) supplemented with 10% FBS, 2 mM L-glutamine, 100 U/ml penicillin, 100 µg/ml streptomycin, and 100 µg/ml zeocin. Flp-in HEK293 cells stably transfected with hPMAT or hOCT3 were maintained in Dulbecco's modified Eagle's medium (high glucose) supplemented with 10% FBS, 2 mM L-glutamine, 100 U/ml penicillin, 100 µg/ml streptomycin, and 150 µg/ml hygromycin. Cells were cultured in a 37°C humidified incubator with 5% CO₂. For better attachment of cells, all cell culture plastic surfaces were pretreated with 0.01% poly L-ornithine (molecular weight ~30,000–70,000)/phosphate-buffered saline solution before plating.

Generation of HEK293 Cell Lines Stably Expressing hPMAT and hOCT3 at Isogenic Locations. To generate HEK293 cell lines stably expressing hPMAT or hOCT3 at isogenic locations, the Flp-in system from Invitrogen was used. This system uses Flp-recombinase to mediate integration of the transfected gene into the flippase recognition target (FRT) site in the Flp-in host cells. hPMAT (SLC29A4) cDNA was cloned previously (Engel et al., 2004). It was amplified by using Pfu Ultra polymerase (Stratagene, La Jolla, CA) with the primers 5'-TATGGATCCGAGAGGCTGCCATGGGCTCCGT-3' and 5'-AATGCGGCCAGTGGGCGGGCTGGCTCAGA-3' and ligated into the BamHI/NotI sites of pcDNA5/FRT vector (Invitrogen). To clone hOCT3 (SLC22A3) cDNA, human skeletal muscle total RNA (Clontech, Mountain View, CA) was reverse-transcribed by using Superscript III reverse transcriptase (Invitrogen) according to the manufacturer's instruction. hOCT3 cDNA was amplified from the cDNA pool with the primers 5'-AATAGGATCCCGCACCATGCCCTCCTTC-GACGA-3' and 5'-GAGGCTCGAGTCTGGATAGCTCCTTCTTC-TGTC-3' and ligated into the BamHI/XhoI sites of pcDNA5/FRT vector. Inserts of both hPMAT and hOCT3 expression vectors were sequenced and aligned with National Center for Biotechnology Information reference sequences (AY485959.1 and NM_021977.2) to ensure fidelity. The encoded amino acid sequences of hPMAT and hOCT3 are identical to the published protein sequences (Kekuda et al., 1998; Engel et al., 2004). The pcDNA5/FRT empty vector and hPMAT or hOCT3 expression vectors were then cotransfected with pOG44 expressing the Flp-recombinase into the Flp-in HEK293 cell line from Invitrogen, which contains only one FRT site at a defined genomic locus. Transfected cells were selected by hygromycin B treatment (150 µg/ml) and expanded. All stably transfected cell lines were cultured in the presence of hygromycin B (150 µg/ml), and cells of 10 to 30 passages were used for this study.

Immunostaining of Flp-in hPMAT and hOCT3 Cell Lines. Flp-in hPMAT and hOCT3 cells were grown on Lab-Tek II CC2 Chamber Slide System (Nalgene Nunc International, Rochester, NY) pretreated with poly L-ornithine for ~2 to 3 days until confluent. Cells were rinsed twice with Dulbecco's phosphate-buffered saline (DPBS) and fixed for 30 min at room temperature with 4% paraformaldehyde, rinsed twice with DPBS, and incubated in 50 mM NH₄Cl in DPBS for 15 min to quench the fixative. Cells were then perme-

abilized with 0.2% Triton X-100 in DPBS for 10 min followed by 90-min incubation with blocking buffer (10% FBS, 0.1% Triton X-100 in DPBS) to block nonspecific binding sites. Cells were incubated with primary antibodies diluted in blocking buffer overnight at 4°C with constant shaking. We previously reported PMAT polyclonal antibody directed against the C-terminal amino acids 469 to 482 of human PMAT protein (Dahlin et al., 2007) and diluted 1:200. OCT3 polyclonal antibody (C-14) was obtained from Santa Cruz Biotechnology, Inc. (Santa Cruz, CA) and used at 1:100 dilution. After incubating with primary antibodies, cells were washed three times with DPBS containing 0.05% Triton X-100 and incubated with fluorescence-conjugated secondary antibodies for 1 h (Alexa Fluor 488 goat anti-rabbit for PMAT, Alexa Fluor 555 donkey anti-goat for OCT3, both from Invitrogen, and diluted 1:1000 in blocking buffer). Cells were washed three times and observed under a Nikon (Tokyo, Japan) fluorescence microscope with imaging capabilities.

Taqman Real-Time RT-PCR for Quantification of hPMAT and hOCT3 mRNA Transcripts. Flp-in HEK293 cells total RNA were extracted by using a RNeasy minikit (QIAGEN, Valencia, CA). Total RNA from various human tissues were purchased from Clontech. The RNA samples were prepared from normal nondiseased human tissues pooled from varying numbers of subjects (see Supplemental Table 1 for details). Total RNA (~2–4 µg) was reverse-transcribed to first-strand cDNA using Superscript III reverse transcriptase (Invitrogen) according to the manufacturer's protocol. Taqman real-time PCR reagents, supplies, primers, and probes for hPMAT (SLC29A4), hOCT3 (SLC22A3), and β-glucuronidase (GUSB) were purchased from Applied Biosystems (Foster City, CA). All primers and probes for cDNAs were validated by Applied Biosystems. The primers were designed to span adjacent exons so that genomic DNA would not be amplified (hPMAT and hOCT3, exons 9–10; GUSB, exons 11–12). Taqman real-time PCRs were set up and run according to the manufacturer's protocols on an Applied Biosystems 7900HT fast real-time PCR system. Ten to 100 ng of cDNA was used per well in a total volume of 25 µl on a 96-well, clear-top, real-time PCR plate. All samples were run in triplicate. For absolute quantification, standard curves for hPMAT and hOCT3 were generated on each plate by using serial dilutions of the cDNA expression vectors with predetermined copy numbers. For relative quantification, GUSB standard curve was generated by using serial dilutions of Flp-in HEK293 cell cDNA. GUSB was selected as the reference gene because previous reports suggested its expression level is more stable than other commonly used housekeeping genes such as β-actin and glyceraldehyde-3-phosphate dehydrogenase (Fink et al., 2008; Romanowski et al., 2008). Absolute or relative amounts for each cDNA were calculated by plotting Log(amount) against Ct (threshold cycle) values on a semilog plot. A linear relationship between Log(amount) and Ct was indicated by each standard curve.

Uptake Assays in Cultured Cells. Flp-in pcDNA5 control cells and hPMAT and hOCT3 cells were plated in 24-well plates and allowed to grow for ~2 to 3 days to reach ~80 to 90% confluence. Transport assays were performed at 37°C in KRH buffer (5.6 mM glucose, 125 mM NaCl, 4.8 mM KCl, 1.2 mM KH₂PO₄, 1.2 mM CaCl₂, 1.2 mM MgSO₄, 25 mM HEPES, pH 7.4) containing known concentrations of substrates with radiolabeled tracer compounds. Uptake was terminated by washing the cells three times with ice-cold KRH buffer. Cells were then solubilized with 0.5 ml of 1 N NaOH at 37°C for 2 h and neutralized with 0.5 ml of 1 N HCl, and 0.4 ml of the lysates was used for liquid scintillation counting. Protein concentrations in the lysates were measured by using a BCA protein assay kit (Pierce Chemical, Rockford, IL), and the uptake in each well was normalized to its protein content. Transporter-specific uptake was calculated by subtracting the background uptake in Flp-in pcDNA5 cells. All uptake assays were performed in triplicate.

Synaptosome Preparation and Uptake Experiments. Mouse brain synaptosomes were prepared by using a method described by

Zhu et al. (2006). In brief, adult mice of both sexes (2–4 months old) were euthanized in a CO₂ chamber. Whole brain was quickly removed and homogenized on ice in a homogenizer (Wheaton Science Products, Millville, NJ) with 5 ml of ice-cold sucrose homogenization buffer (320 mM sucrose, 5 mM HEPES, pH 7.4). The homogenate was centrifuged at 1000g, 4°C for 10 min to remove nuclear debris. The supernatant was centrifuged again at 16,000g, 4°C for 20 min. The synaptosome pellet was washed twice in 20 ml of ice-cold synaptosome uptake buffer (130 mM NaCl, 10 mM D-glucose, 1.3 mM KCl, 2.2 mM CaCl₂, 1.2 mM MgSO₄, 1.2 mM KH₂PO₄, 10 mM HEPES, 0.1 mM ascorbate, pH 7.4) and resuspended in 6 ml of uptake buffer. For uptake assays, 100 µl of synaptosome preparations was preincubated with 100 µl of synaptosome uptake buffer with or without inhibitors for 10 min in a 37°C shaking water bath. To initiate the uptake, 100 µl of monoamine substrates spiked with [³H]radiolabeled tracers was added to the synaptosomes. The final concentrations of all monoamine substrates were 0.5 µM. The inhibitors used in the uptake buffer were citalopram (10 µM), 1-[2-bis(4-fluorophenyl)methoxyethyl]-4-(3-phenylpropyl)piperazine (GBR12909) (1 µM), desipramine (1 µM), decynium-22 (10 µM), and corticosterone (100 µM). After 5-min incubation at 37°C with gentle shaking, the uptake was terminated by diluting the synaptosome mixture in 5 ml of ice-cold uptake buffer, followed immediately by filtration through Whatman (Clifton, NJ) GF/B glass microfiber filters on a vacuum filtration manifold. The filters were then washed with ice-cold uptake buffer, transferred to scintillation vials, and immersed in scintillation fluid overnight before counting. Nonspecific monoamine binding to filters was obtained by setting up parallel assays without adding synaptosomes. Specific monoamine uptake of synaptosomes was calculated by subtracting nonspecific binding counts.

Data Analysis. Data points with error bars indicate mean ± S.D. for independent triplicates. All experiments were repeated approximately two to three times. Where applicable, *p* values were obtained through Student's *t* test. Data groups are considered significantly different if *p* < 0.05. The kinetics data were fitted in Prism software (GraphPad Software Inc., San Diego, CA) with the Michaelis-Menten equation $V = V_{\max} \times S / (K_m + S)$, where *V* is specific uptake rate, *S* is substrate concentration, *V*_{max} is the maximal uptake rate, and *K*_m is the Michaelis constant. All data obtained good fittings with *R*² > 0.95.

Results

Stable Expression of hOCT3 and hPMAT in Flp-in HEK293 Cells. To directly compare the intrinsic transport efficiency (*V*_{max}/*K*_m) of hOCT3 and hPMAT toward monoamines, it is important to know the protein expression level of each transporter in the system. This is because the *V*_{max} measured from cell uptake studies is a product of intrinsic catalytic efficiency (*K*_{cat}) of a single transporter and the number of transporters (*E*_{total}) in the system (i.e., *V*_{max} = *K*_{cat} × *E*_{total}). Currently, there are no methods to directly quantify the amount of hOCT3 or hPMAT expressed on the cell surface. Because of the lack of purified hOCT3 or hPMAT protein as a normalization standard, it is also not feasible to quantify protein expression by using immunoblotting methods. One approach to overcome this problem is to generate cell lines that express these transporters at similar levels so that the *V*_{max} values are directly comparable with each other to infer their intrinsic transport efficiency. To this end, we chose the Flp-in system that uses Flp recombinase to integrate an expressed gene into a defined genomic locus (Weichert et al., 2006; Nourian et al., 2008). The commercially supplied Flp-in HEK293 cell line is engineered to contain a

single integration site. Stably transfected cells contain only a single copy of the transporter cDNA integrated at the same genomic locus and under the control of the same cytomegalovirus promoter, resulting in consistent and comparable expression of the transfected gene. After transfection and hygromycin selection, we obtained stable cell lines for hOCT3 and hPMAT. Taqman real-time PCR was used to quantify the copy numbers of hOCT3 and hPMAT transcripts in the two cell lines. As shown in Fig. 1A, hOCT3 and hPMAT transcripts were expressed at similar levels in the two transfected cell lines. Endogenous expression of hOCT3 and hPMAT mRNA in HEK293 cells was negligible (data not shown). Immunostaining with hOCT3- or hPMAT-specific antibodies showed that the corresponding transporters were expressed on plasma membranes with uniform distribution in nearly every cell (Fig. 1B). Because some background staining was observed for OCT3 immunostaining in control cells, additional Western blot analysis was performed. The data confirmed that the hOCT3 protein was specifically expressed in hOCT3 cDNA-transfected, but not pcDNA5 vector-transfected, cells (Supplemental Fig. 1). To evaluate the expression stability with culture time, MPP⁺ (1 μ M) uptake activity was measured in all subsequent uptake assays using cells of 10 to 30 passages. In all uptake experiments, absolute MPP⁺ transport rates were consistent with no more than 20% batch-to-batch variations (data not shown). These data suggest that we have obtained two human cell lines that stably express hOCT3 and hPMAT at similar levels on the cell surface.

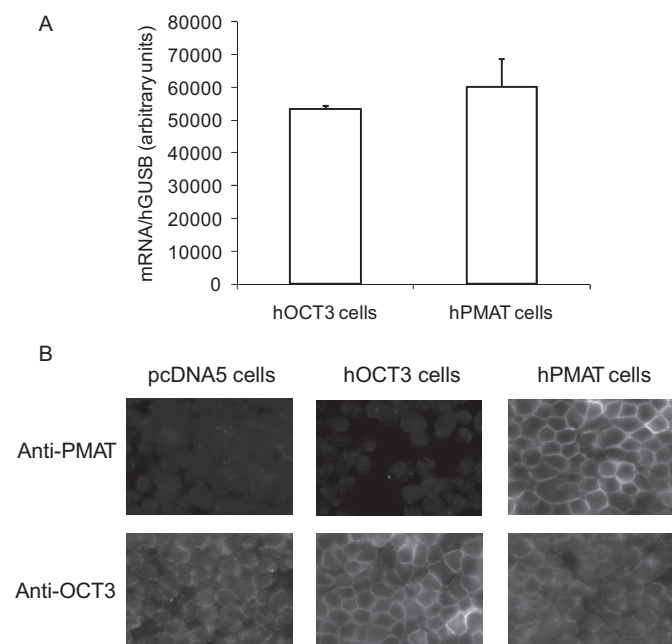


Fig. 1. A, quantification of hOCT3 and hPMAT mRNA levels in stably transfected Flp-in HEK293 cells. Total RNA from Flp-293-pcDNA5, hOCT3, and hPMAT cells were extracted and reverse-transcribed. hOCT3 and hPMAT mRNA copy numbers were determined by Taqman real-time RT-PCR using specific primers and probes. Diluted hOCT3 and hPMAT expression vectors with known copy numbers were used as standards to determine absolute mRNA copy numbers. B, localization of hOCT3 and hPMAT in Flp-in HEK293 cells stably transfected with hPMAT or hOCT3. Cells transfected with pcDNA5 vector were used as control. Confluent cells were immunostained with anti-OCT3 or anti-PMAT primary antibodies and Alexa Fluor-conjugated secondary antibodies. Images were taken under a fluorescent microscope with corresponding filters.

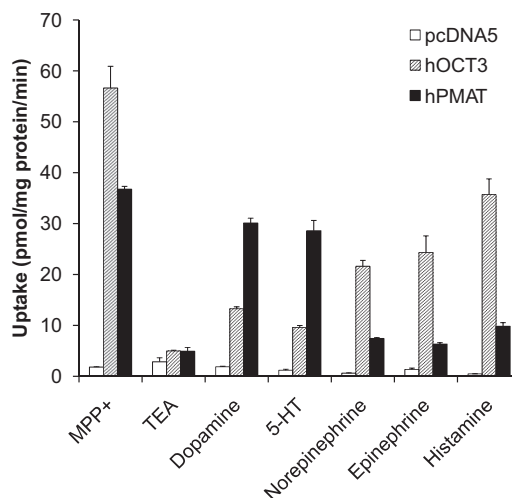


Fig. 2. Uptake of MPP⁺, TEA, and monoamines by hOCT3 and hPMAT. Flp-293 pcDNA5, hOCT3, and hPMAT cells were run in parallel with substrate concentrations at 1 μ M.

Monoamine Uptake by hOCT3 and hPMAT. To assess the activity of hOCT3 and hPMAT in the stable cell lines, parallel uptake was carried out in vector control, hOCT3, and hPMAT cells for endogenous monoamines (5-HT, dopamine, norepinephrine, epinephrine, histamine) and two model organic cations (MPP⁺ and TEA). All compounds were used at a final concentration of 1 μ M. Compared with vector-transfected cells, significantly enhanced uptake was observed for all seven tested compounds in both hOCT3- and hPMAT-expressing cells (Fig. 2). Both transporters demonstrated a high activity toward MPP⁺ but a very low activity for TEA. For the endogenous amines, the transport activities of hOCT3 were higher for histamine, epinephrine, and norepinephrine than for dopamine and 5-HT. For hPMAT, an opposite pattern showing higher dopamine and 5-HT transport activity was observed.

Transport Kinetics. To determine the kinetic basis for the differential uptake activity of hOCT3 and hPMAT, initial rate studies were carried out. To define the initial rate period for each substrate, time-dependent uptake was first carried out. The initial phase, where uptake rates increase linearly with time, varied for the test compounds and lasted approximately 2 to 5 min (Fig. 3). Uptake was linear within 2 min for all compounds, and 2-min incubation time was therefore used in kinetic studies except for TEA. Because of the low TEA uptake activities for both hOCT3 and hPMAT, TEA kinetic study was extended to 5 min, which is still within the linear range (Fig. 3), to increase signal-to-noise ratio. Metabolism of monoamines was also negligible because the monoamine oxidase inhibitor pargyline (10 μ M) had no effect on uptake rates (data not shown).

We then performed parallel kinetic analysis for each substrate in vector and hOCT3- and hPMAT-expressing cells. Specific uptake was obtained by subtracting background uptake in vector-transfected cells. The data were fitted to the Michaelis-Menten equation (Fig. 4), and the kinetic parameters are summarized in Tables 1 and 2. For MPP⁺, a probe substrate transported by all organic cation transporters, hOCT3 and hPMAT showed similar apparent binding affinity ($K_m = 166 \pm 11$ versus 111 ± 3 μ M), but the V_{max} was

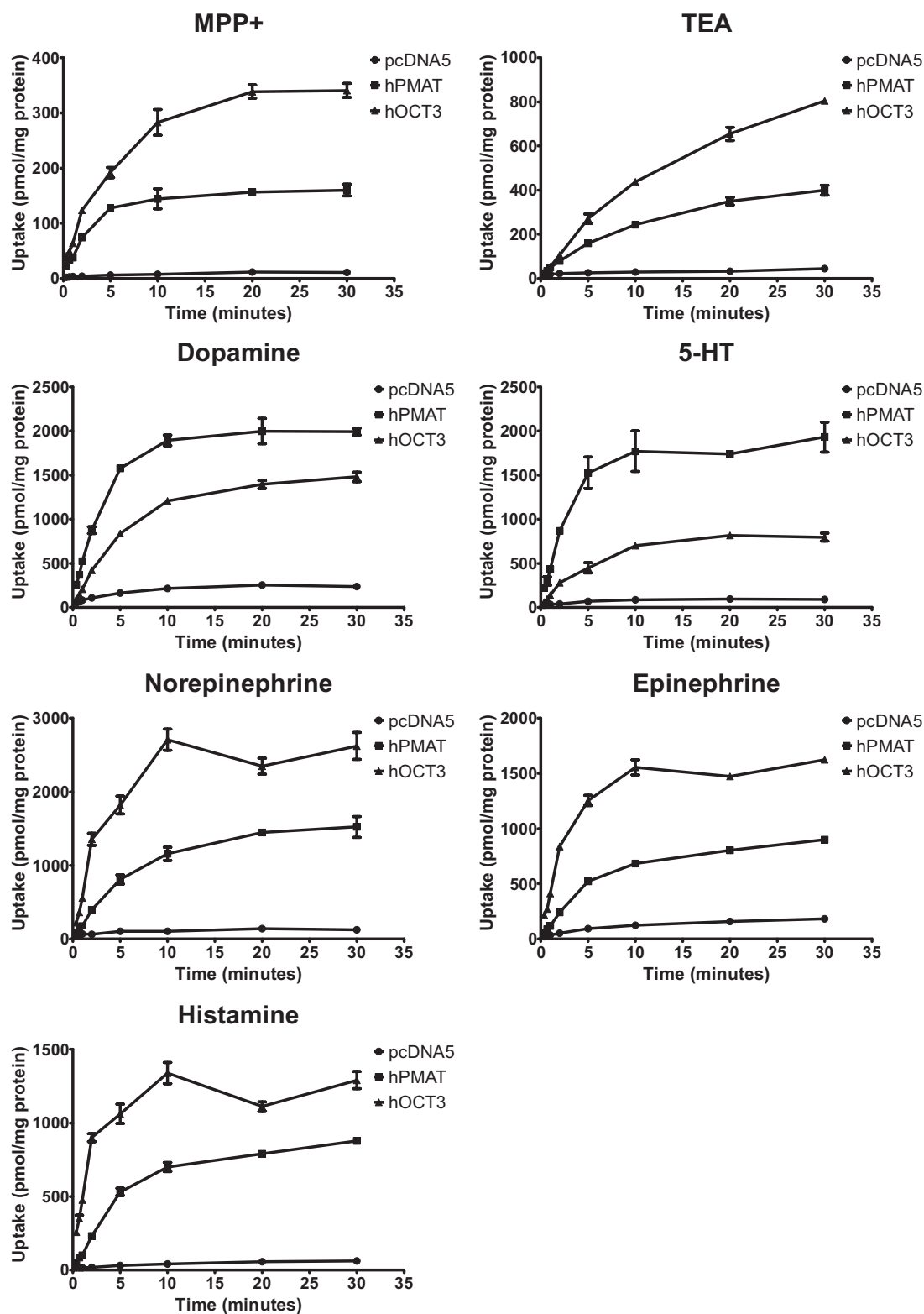


Fig. 3. Time-dependent uptake of MPP⁺, TEA, and monoamines by hOCT3 and hPMAT. Uptake experiments were conducted as described under *Materials and Methods* for up to 30 min. Time points were chosen within the linear uptake phases (which range between 2 and 5 min) to determine kinetics parameters. The concentrations of substrates were: MPP⁺, 1 μ M; dopamine, 10 μ M; 5-HT, 10 μ M; norepinephrine, 20 μ M; epinephrine, 20 μ M; histamine, 10 μ M; TEA, 20 μ M.

somewhat higher for hOCT3, resulting in ~ 2 -fold higher transport efficiency (V_{\max}/K_m) than hPMAT. For TEA, the V_{\max}/K_m values were similar between the two transporters, and the transport efficiency was only 3% of their transport

efficiency toward MPP⁺. It is noteworthy that the mechanism underlying the low TEA transport efficiency seems to be different. For hPMAT, this was mainly caused by a much reduced affinity (80-fold lower) in spite of a 2-fold increase in

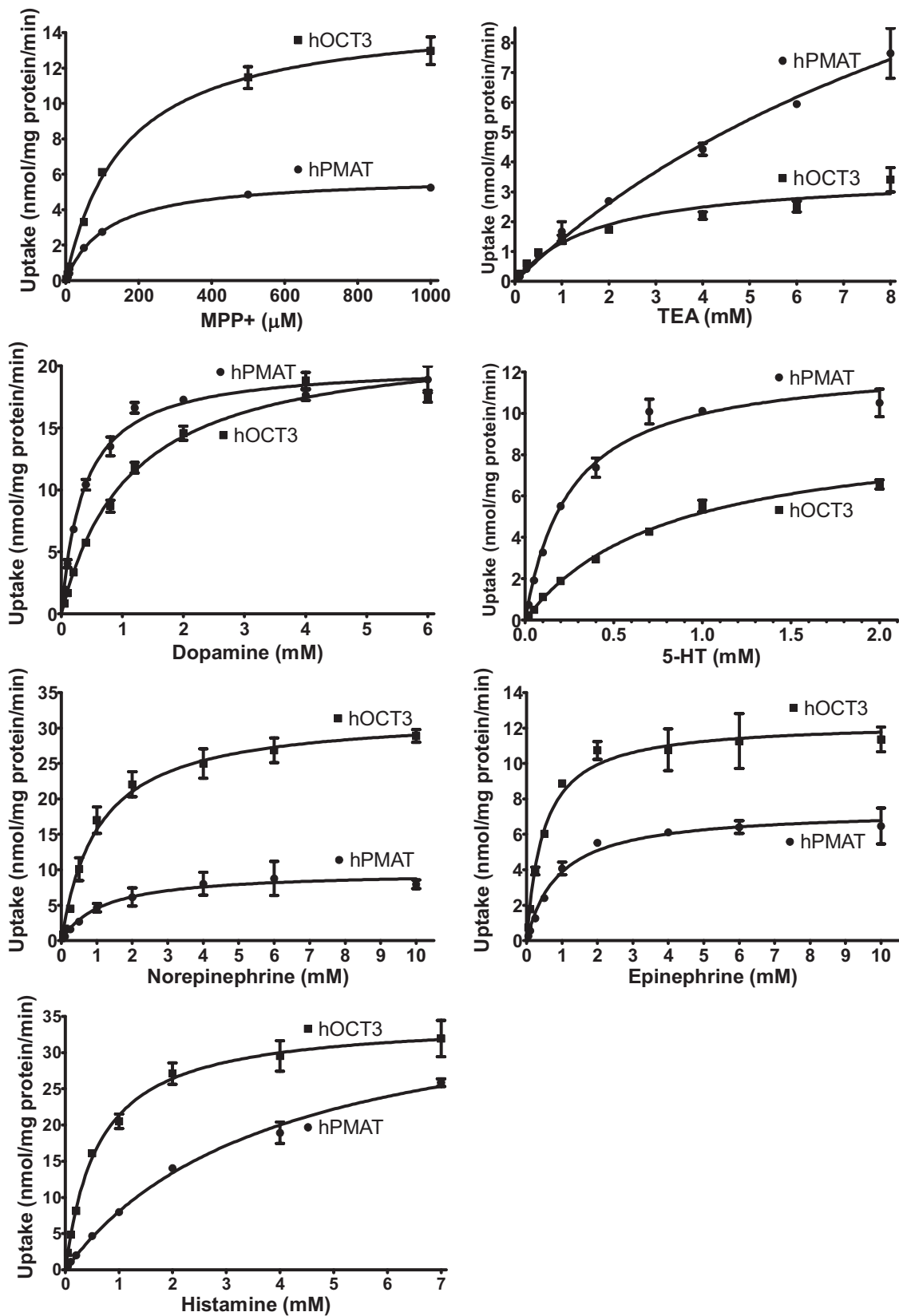


Fig. 4. Concentration-dependent uptake for MPP+, TEA, and monoamines in hOCT3 and hPMAT cells. Uptake for a specific substrate was carried out in parallel in Flp-293 pcDNA5, hOCT3, and hPMAT cells. Uptake in pcDNA5 cells were subtracted from hOCT3 or hPMAT cells to obtain transporter-specific uptake. Uptake time points were 5 min for TEA and 2 min for all other substrates.

TABLE 1

Summary of kinetic parameters for hOCT3

Concentration-dependent uptake for MPP⁺, TEA, and monoamines was carried out in parallel in Flp-293 pcDNA5 and hOCT3 cells. Uptake in pcDNA5 cells was subtracted from hOCT3 cells to obtain hOCT3-specific uptake. Uptake time points were 5 min for TEA and 2 min for all other substrates. The kinetics data were fitted in GraphPad Prism software with the Michaelis-Menton equation. Data represent mean \pm S.D. for two to three independent experiments.

Substrate	K_m	V_{max}	V_{max}/K_m	V_{max}/K_m Relative to MPP+
	μM	$pmol/mg\ protein/min$	$\mu l/mg\ protein/min$	%
MPP+	166 \pm 11	15,664 \pm 821	94.7 \pm 1.1	100
TEA	921 \pm 161	2760 \pm 92	3.03 \pm 0.43	3.2
Dopamine	1033 \pm 127	22,676 \pm 484	22.1 \pm 3.2	23
5-HT	988 \pm 264	11,562 \pm 3109	11.7 \pm 0.2	12
Norepinephrine	923 \pm 172	30,134 \pm 2674	32.9 \pm 1.3	35
Epinephrine	458 \pm 37	12,760 \pm 605	28.0 \pm 3.6	30
Histamine	641 \pm 24	34,604 \pm 47	54.0 \pm 2.1	57

TABLE 2

Summary of kinetic parameters for hPMAT

Concentration-dependent uptake for MPP⁺, TEA, and monoamines was carried out in parallel in Flp-293 pcDNA5 and hPMAT cells. Uptake in pcDNA5 cells was subtracted from hPMAT cells to obtain hPMAT-specific uptake. Uptake time points were 5 min for TEA and 2 min for all other substrates. The kinetics data were fitted in GraphPad Prism software with the Michaelis-Menton equation. Data represent mean \pm S.D. for two to three independent experiments.

Substrate	K_m	V_{max}	V_{max}/K_m	V_{max}/K_m Relative to MPP+
	μM	$pmol/mg\ protein/min$	$\mu l/mg\ protein/min$	%
MPP+	111 \pm 3	6557 \pm 942	59.2 \pm 10.0	100
TEA	8759 \pm 3175	15,246 \pm 3023	1.79 \pm 0.30	3.0
Dopamine	406 \pm 48	22,402 \pm 3166	55.1 \pm 1.3	93
5-HT	283 \pm 40	14,194 \pm 2381	50.1 \pm 1.4	85
Norepinephrine	1078 \pm 107	8822 \pm 1323	8.16 \pm 0.41	14
Epinephrine	951 \pm 59	7252 \pm 195	7.65 \pm 0.68	13
Histamine	4379 \pm 679	42,374 \pm 4098	9.72 \pm 0.57	16

V_{max} . However, for hOCT3, a reduced (5.7-fold) V_{max} and a lower affinity (5.5-fold) both contributed.

For the endogenous monoamines, a seemingly complementary pattern was observed. For hOCT3, the rank order of V_{max}/K_m is histamine > norepinephrine, epinephrine > dopamine > 5-HT (Table 1). For hPMAT, the V_{max}/K_m rank order is dopamine, 5-HT \gg histamine, norepinephrine, epinephrine (Table 2). Compared with hOCT3, hPMAT is much more selective toward 5-HT and dopamine because its V_{max}/K_m for these two amines is five to seven times greater than other amines. In contrast, only 2- to 4.6-fold difference in V_{max}/K_m was observed for hOCT3 for its favored versus unfavored amines (Table 1). It is noteworthy that, like TEA, the mechanisms underlying the monoamine selectivity of hOCT3 and hPMAT seemed quite different. For hPMAT, a distinction in K_m was a primary driving force, and the transporter displayed up to 15-fold differences in K_m but no more than 3-fold differences in V_{max} for its favored amines (dopamine, 5-HT) versus the unfavored ones (histamine, norepinephrine, epinephrine) (Table 2). In contrast to hPMAT, the substrate preference of hOCT3 was not readily observable in its apparent binding affinity (K_m), because the transporter exhibited no more than 2-fold differences in its K_m values toward all amines. Differences in V_{max} contributed significantly in determining the monoamine preference (as measured by V_{max}/K_m) of hOCT3 (Table 1).

Quantification of hPMAT and hOCT3 Transcripts in Various Human Tissues and Brain Regions. Our analysis in the heterologous expression system revealed distinct transport kinetic properties of hPMAT and hOCT3 toward endogenous monoamines. The relevance of these two transporters in clearing a specific monoamine in vivo will depend on their intrinsic transport efficiency for the amine and the abundance of the transporter in the relevant tissue. Using

Taqman real-time PCR assay, we quantified the copy numbers of hPMAT and hOCT3 transcripts in mRNA pooled from normal human tissues (see Supplemental Table 1 for details). The absolute copy numbers of hPMAT and hOCT3 mRNA in 10 ng of total RNA and their relative levels normalized to GUSB are shown in Fig. 5. In the nine tested human brain areas, hPMAT expression in general was much higher than hOCT3. hPMAT transcripts are particularly abundant in the cerebral cortex, hippocampus, substantia nigra, medulla oblongata, and cerebellum. In the peripheral organs, adrenal gland and skeletal muscle highly and selectively expressed hOCT3, whereas pancreas selectively expressed hPMAT. In heart and small intestine, the two transporters were expressed at similar levels.

Monoamine Uptake in Mouse Brain Synaptosomes.

To further explore the relevance of PMAT and OCT3 in brain monoamine uptake, we examined the uptake of the monoamine neurotransmitters 5-HT, dopamine, and norepinephrine in synaptosomes prepared from mouse whole brain homogenates. To reveal uptake₂ activities, the following well established specific inhibitors were used to suppress uptake₁ transporters: citalopram for SERT (Torres et al., 2003), GRB12909 for DAT (Andersen, 1989), and desipramine for NET (Bymaster et al., 2002). Previous studies demonstrated that D22 is a potent inhibitor for both human PMAT and OCT3, whereas corticosterone potently inhibits OCT3 but not PMAT (Gründemann et al., 1998; Hayer-Zillgen et al., 2002; Engel et al., 2004). The concentrations of the inhibitors were chosen based on their reported K_i or IC_{50} values, and their effects on PMAT and OCT3 were first tested in the stably transfected cells. As expected, the uptake₁ inhibitors citalopram (10 μM), GBR12909 (1 μM), and desipramine (1 μM) had negligible effect (less than 10% inhibition) on hPMAT- or

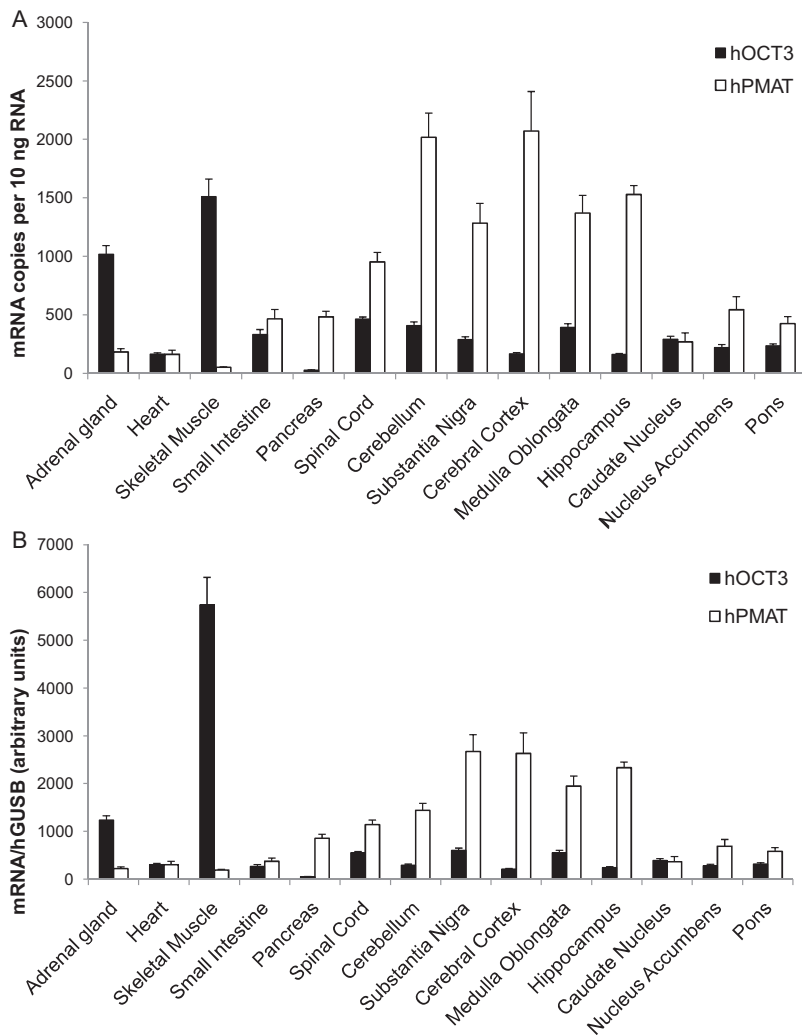


Fig. 5. hOCT3 and hPMAT mRNA levels in various human tissues and brain regions. Total RNA from human tissues were reverse-transcribed to cDNA. hOCT3, hPMAT, and hGUSB transcripts levels were quantified by using Taqman real-time RT-PCR. A, absolute copy numbers of hOCT3 and hPMAT mRNA in 10 ng of total RNA. B, hOCT3 and hPMAT mRNA levels normalized to hGUSB.

hOCT3-mediated MPP⁺ uptake (Fig. 6). On the other hand, corticosterone (100 μ M) almost completely suppressed hOCT3 activity without affecting PMAT. D22 (10 μ M) effec-

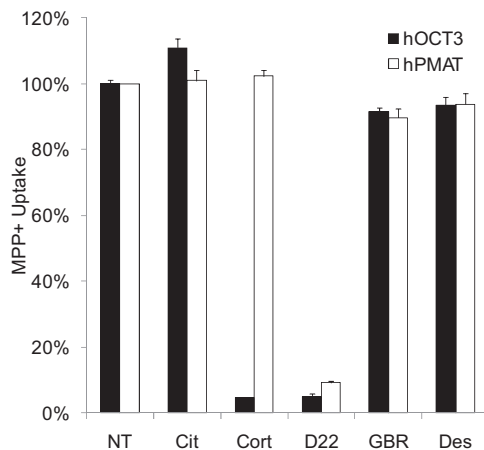


Fig. 6. Effects of inhibitors used in synaptosome uptake studies on MPP⁺ uptake mediated by hOCT3 and hPMAT. Flp-293 pcDNA5, hOCT3, and hPMAT cells were run in parallel with MPP⁺ concentrations at 1 μ M and in the absence or presence of inhibitors. NT, no treatment; Cit, citalopram (10 μ M); Cort, corticosterone (100 μ M); D22 (10 μ M); GBR, GBR12909 (1 μ M); Des, desipramine (1 μ M). Data are expressed as percentage of MPP⁺ uptake obtained from cells with no treatment.

tively inhibited both hOCT3 and hPMAT (Fig. 6). These results were consistent with previous reports and justified the concentrations of the inhibitors used in our synaptosome uptake studies. We then examined the uptake of the monoamine neurotransmitters 5-HT, dopamine, and norepinephrine in mouse brain synaptosomes. As shown in Fig. 7A, citalopram reduced synaptosome 5-HT uptake by ~50%, consistent with SERT playing a major role in brain 5-HT clearance. Coinhibition of citalopram with D22 inhibited 5-HT uptake by ~70%, suggesting that non-SERT-mediated 5-HT uptake may account for 20% of total synaptosome uptake. We were surprised to find that D22 alone inhibited 5-HT uptake by 60%, suggesting that D22 may also substantially affect SERT at the concentration used. In contrast, corticosterone had no effect on synaptosome 5-HT uptake. Similar inhibitory patterns were obtained for dopamine and norepinephrine uptake (Fig. 7, B and C). The DAT inhibitor GBR12909 inhibited synaptosomal dopamine uptake by more than 50%. D22 alone inhibited dopamine uptake by 65%. Coinhibition of D22 with GBR12909 produced 85% inhibition. Corticosterone, alone or with GBR12909, had no specific or additive effect. For norepinephrine (Fig. 7C), the NET inhibitor desipramine inhibited synaptosomal norepinephrine uptake by approximately 45%. D22 alone only inhibited norepinephrine uptake by approximately 25%. Coinhibition of desipramine

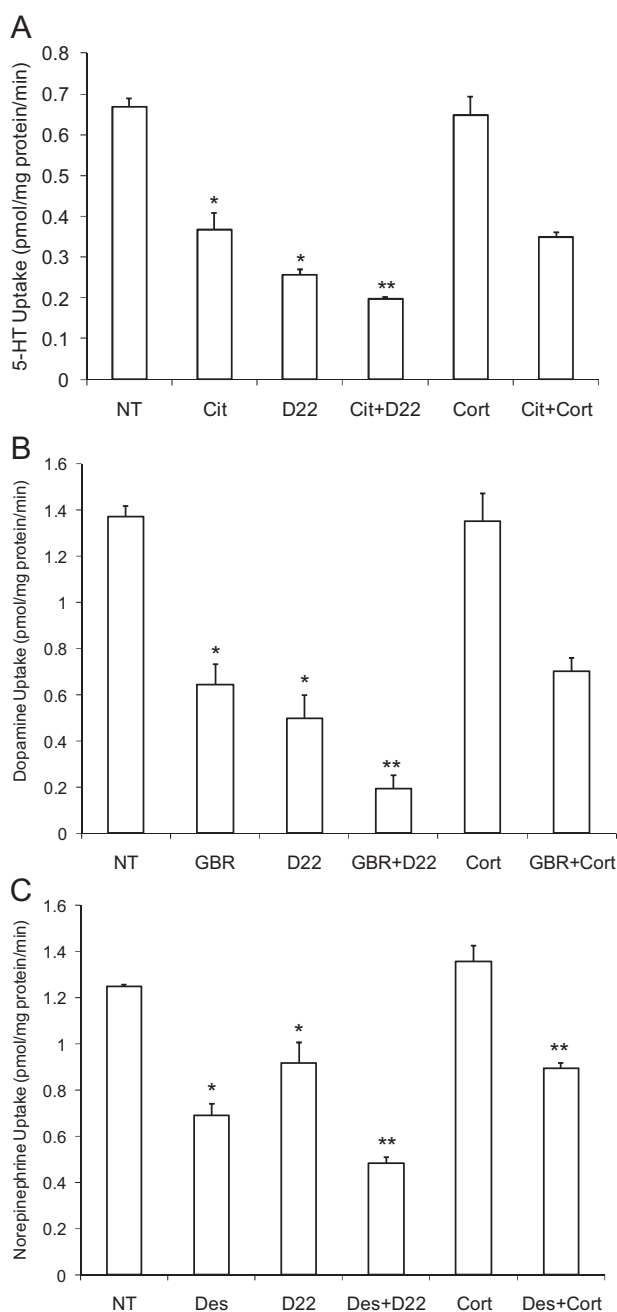


Fig. 7. Uptake of 0.5 μM 5-HT (A), dopamine (B), and norepinephrine (C) in adult mouse brain synaptosomes in the presence or absence (no treatment) of various inhibitors. Cit, citalopram (10 μM); Cort, corticosterone (100 μM); D22 (10 μM); GBR, GBR12909 (1 μM); Des, desipramine (1 μM). *, $p < 0.05$ compared with no treatment (NT); **, $p < 0.05$ compared with citalopram, GBR12909, or desipramine alone.

with D22 produced 60% inhibition. Corticosterone still had no effect on norepinephrine uptake.

Discussion

The removal of released monoamine neurotransmitters through transporters is a major mechanism to inactivate the chemical messengers. Studies suggest that, in addition to the high-affinity, low-capacity uptake₁ transporters, low-affinity, high-capacity uptake₂ transporters play a significant role in regulating monoamine neurotransmission (Iversen, 1971;

Eisenhofer, 2001). Uptake₂ transporters (e.g., PMAT and OCT3) may represent promising drug targets for neuropsychiatric disorders (Schildkraut and Mooney, 2004; Zhou et al., 2007; Daws, 2009). However, before these transporters can be further explored as drug targets, it is crucial to know the relative contribution of PMAT and OCT3 in clearing specific monoamines in vivo, which is directly related to their intrinsic transport efficiencies and expression levels at the physiological sites of interest.

The transport activities of OCT3 or PMAT toward monoamines have been evaluated previously in several discrete studies (Gründemann et al., 1998, 1999; Engel et al., 2004; Engel and Wang, 2005; Amphoux et al., 2006). However, results from these studies are difficult to compare because transporter expression levels vary in different systems and kinetic data are not available for some monoamines. Furthermore, discrepancies exist in published data. For example, the reported K_m of hOCT3 for norepinephrine varied more than 5-fold (Gründemann et al., 1998; Amphoux et al., 2006; Koepsell et al., 2007), probably because of prolonged incubation time used in some studies. Therefore, in the current study, we aimed to comprehensively and rigorously analyze the transport kinetics of hOCT3 and hPMAT toward monoamines under well controlled conditions.

Using the Flp-in system, we isogenically expressed hPMAT and hOCT3 in HEK293 cell lines at comparable transcript levels (Fig. 1). During the course of our study, the transport activities of both hPMAT and hOCT3 were stable as measured by MPP⁺ uptake (<20% variation; data not shown). All studies were done at a short incubation time within the linear range (Fig. 3). Our analysis revealed complementary substrate preference of hPMAT and hOCT3 for the monoamine neurotransmitters. hPMAT exhibits strong preference for dopamine and 5-HT, whereas hOCT3 favors histamine, norepinephrine, and epinephrine. The two transporters differ markedly in their magnitudes of selectivity. The V_{max}/K_m values of hPMAT for 5-HT and DA are five to seven times greater than for other monoamines (Table 2). In contrast, hOCT3 shows only 2- to 4.6-fold difference in V_{max}/K_m for monoamines. The mechanisms underlying their selectivity are also different. For hPMAT, the substrate preference is readily observable in its K_m , suggesting that initial substrate binding is an important step for hPMAT selectivity. In contrast, hOCT3 exhibits less than 2-fold variations in its K_m values toward various monoamines. Distinction in V_{max} contributes significantly to differences in V_{max}/K_m , suggesting that turnover rates are more important in the monoamine selectivity of hOCT3. MPP⁺ and TEA are two probe substrates for all organic cation transporters (Koepsell et al., 2007). MPP⁺ is efficiently transported by hOCT3 and hPMAT with comparable K_m . It is noteworthy that hPMAT transports dopamine and 5-HT almost as effectively as MPP⁺ (Table 2). hOCT3, however, transports its most favored monoamine, histamine, only at 50% efficiency of MPP⁺. We also found that TEA is a poor substrate for both hOCT3 and hPMAT with transport efficiencies only 3% of that of MPP⁺.

The complementary kinetic profiles of hPMAT and hOCT3 suggest that the two transporters may have distinct functions in monoamine uptake in vivo. To further evaluate the roles of these transporters in vivo, we quantified the mRNA copy numbers in selected human tissues and brain regions by

real-time RT-PCR (Fig. 5). In the CNS, hPMAT transcripts significantly outnumber hOCT3 in eight of the nine tested regions, suggesting that hPMAT is the major uptake₂ transporter in the CNS. Consistent with our previous findings in mouse brain (Dahlin et al., 2007), hPMAT is highly expressed in brain areas innervated with serotonergic and dopaminergic fibers such as the cerebral cortex, hippocampus, substantia nigra, and cerebellum. However, contrary to our previous Northern blot data, which showed high hPMAT hybridization signal in skeletal muscle (Engel et al., 2004), we detected only low expression of hPMAT in this tissue by real-time RT-PCR. The reason for this discrepancy could be interindividual variations in gene expression. In addition, our previous study may have overestimated the abundance of hPMAT in skeletal muscle because the mRNA loading control (β -actin) was overly saturated in that study. Similar to this study, we did not detect significant expression of Pmat in mouse skeletal muscle (Dahlin et al., 2007). Our results showed that hOCT3 is selectively and highly expressed in the adrenal gland and skeletal muscle. The medulla of adrenal gland is the body's major source of circulating epinephrine and norepinephrine, which elicit the fight-or-flight response (Ungar and Phillips, 1983). In the skeletal muscle, adrenergic signaling through α - and β -adrenoceptors controls important physiological functions, including muscle blood flow and metabolism (Lynch and Ryall, 2008). The high expression of hOCT3 in these organs may serve to take up excess circulating epinephrine/norepinephrine after their release.

The apparent affinities of hPMAT and hOCT3 toward the monoamine neurotransmitters are much lower than the uptake₁ transporters. The K_m values of hPMAT and hOCT3 toward monoamines are in the micromolar to millimolar range (Tables 1 and 2) whereas the K_m values of uptake₁ transporters determined in heterologous expression systems are in the submicromolar range (Daws, 2009). The in vivo concentrations of monoamine neurotransmitters fluctuate and vary significantly in different brain areas. The extracellular concentrations of the monoamine are highest at its site of release and plummet as the transmitter diffuses away (Bunin and Wightman, 1999). For example, whereas the concentrations of extracellular 5-HT in mouse striatum and frontal cortex were determined to be in the low nanomolar range by microdialysis (Mathews et al., 2004), its concentration at the synaptic cleft was estimated to be as high as 6 mM (Bunin and Wightman, 1998), which far exceeds the K_m of SERT (0.1–0.4 μ M). Instead, 5-HT is estimated to diffuse more than 20 μ m away from the synaptic cleft, where its concentration falls into the nanomolar range and 5-HT is recycled by SERT localized in the perisynaptic area (Bunin and Wightman, 1998, 1999). Although the precise localization of PMAT or OCT3 in neurons is unknown, it is possible that they participate in the clearance of monoamines at high concentration areas and/or after repeated stimulation of monoaminergic neurons. Clearance by uptake₂ transporters may also predominate when uptake₁ transporters are inactivated pharmacologically, such as under antidepressant treatment. It may not be unusual that the brain uses both high-affinity and low-affinity uptake systems to regulate a wide concentration range of certain endogenous molecules. A recent analysis of *Slc* gene expression in the mouse brain also demonstrated the coexpression of Na⁺-dependent, high-affinity transporters and Na⁺-independent, low-affinity trans-

porters for other endogenous compounds such as choline, nucleosides, and glucose (Dahlin et al., 2009).

As an exploratory study, we also tested the relative contribution of Pmat and Oct3 to monoamine clearance in mouse brain synaptosomes by using chemical inhibitors (Fig. 7). Citalopram, GBR12909, and desipramine reduced synaptosome 5-HT, dopamine, and norepinephrine uptake by approximately 45 to 60%, consistent with uptake₁ transporters playing a major role in brain monoamine clearance. Coinhibition of D22 with uptake₁ inhibitors suppressed monoamine uptake by approximately 60 to 85%, suggesting that uptake₂ activities may account for approximately 15 to 35% of total uptake. The much greater inhibitory effect of D22 alone for 5-HT and dopamine uptake suggests that this compound may also inhibit SERT and DAT to certain degrees. In contrast, the OCT3-specific inhibitor corticosterone had no inhibitory effect on synaptosome uptake of any of the monoamines. These data suggest that PMAT may play a more important role in mediating uptake₂ activities in the brain. However, we can not exclude the role of Oct3 in brain monoamine uptake because there are limitations in the synaptosome uptake studies. Synaptosome studies mainly detect uptake activities in neuronal cells. Oct3 is expressed in astroglial cells (Cui et al., 2009) and could be important for monoamine uptake in these cells. In addition, our studies used synaptosomes prepared from whole brain homogenates and thus may not be able to detect Oct3 activities in specific brain areas or microstructures where its expression is high.

In summary, we examined side-by-side the transport kinetics of hPMAT and hOCT3 for endogenous monoamines in a well controlled expression system. Our data demonstrate complementary substrate preference and distinct tissue expression patterns for hOCT3 and hPMAT. Our results suggest that hPMAT is the major uptake₂ transporter for 5-HT and DA in the CNS, whereas hOCT3 represent the major uptake₂ transporter for histamine, norepinephrine, and epinephrine in peripheral organs. To explore uptake₂ transporters as potential drug targets, the distinct roles of these transporters in human physiology should be considered.

Acknowledgments

We thank Dr. Horace Ho for his contribution to the OCT3 Western blot in Supplemental Fig. 1.

References

- Amara SG and Kuhar MJ (1993) Neurotransmitter transporters: recent progress. *Annu Rev Neurosci* **16**:73–93.
- Amphoux A, Vialou V, Drescher E, Brüß M, Mannoury La Cour C, Rochat C, Millan MJ, Giros B, Bönisch H, and Gautron S (2006) Differential pharmacological in vitro properties of organic cation transporters and regional distribution in rat brain. *Neuropharmacology* **50**:941–952.
- Andersen PH (1989) The dopamine inhibitor GBR 12909: selectivity and molecular mechanism of action. *Eur J Pharmacol* **166**:493–504.
- Blakely RD, De Felice LJ, and Hartzell HC (1994) Molecular physiology of norepinephrine and serotonin transporters. *J Exp Biol* **196**:263–281.
- Bönisch H, Bryan LJ, Henseling M, O'Donnell SR, Stockmann P, and Trendelenburg U (1985) The effect of various ions on uptake₂ of catecholamines. *Naunyn Schmiedeberg's Arch Pharmacol* **328**:407–416.
- Bunin MA and Wightman RM (1998) Quantitative evaluation of 5-hydroxytryptamine (serotonin) neuronal release and uptake: an investigation of extrasynaptic transmission. *J Neurosci* **18**:4854–4860.
- Bunin MA and Wightman RM (1999) Paracrine neurotransmission in the CNS: involvement of 5-HT. *Trends Neurosci* **22**:377–382.
- Bymaster FP, Katner JS, Nelson DL, Hemrick-Luecke SK, Threlkeld PG, Heiligenstein JH, Morin SM, Gehlert DR, and Perry KW (2002) Atomoxetine increases extracellular levels of norepinephrine and dopamine in prefrontal cortex of rat: a potential mechanism for efficacy in attention deficit/hyperactivity disorder. *Neuropsychopharmacology* **27**:699–711.
- Carlsson A (1987) Perspectives on the discovery of central monoaminergic neurotransmission. *Annu Rev Neurosci* **10**:19–40.

- Cui M, Aras R, Christian WV, Rappold PM, Hatwar M, Panza J, Jackson-Lewis V, Javitch JA, Ballatori N, Przedborski S, et al. (2009) The organic cation transporter-3 is a pivotal modulator of neurodegeneration in the nigrostriatal dopaminergic pathway. *Proc Natl Acad Sci USA* **106**:8043–8048.
- Dahlin A, Royall J, Hohmann JG, and Wang J (2009) Expression profiling of the solute carrier gene family in the mouse brain. *J Pharmacol Exp Ther* **329**:558–570.
- Dahlin A, Xia L, Kong W, Hevner R, and Wang J (2007) Expression and immunolocalization of the plasma membrane monoamine transporter in the brain. *Neuroscience* **146**:1193–1211.
- Daws LC (2009) Unfaithful neurotransmitter transporters: focus on serotonin uptake and implications for antidepressant efficacy. *Pharmacol Ther* **121**:89–99.
- Eisenhofer G (2001) The role of neuronal and extraneuronal plasma membrane transporters in the inactivation of peripheral catecholamines. *Pharmacol Ther* **91**:35–62.
- Engel K and Wang J (2005) Interaction of organic cations with a newly identified plasma membrane monoamine transporter. *Mol Pharmacol* **68**:1397–1407.
- Engel K, Zhou M, and Wang J (2004) Identification and characterization of a novel monoamine transporter in the human brain. *J Biol Chem* **279**:50042–50049.
- Fink T, Lund P, Pilgaard L, Rasmussen JG, Duroux M, and Zachar V (2008) Instability of standard PCR reference genes in adipose-derived stem cells during propagation, differentiation and hypoxic exposure. *BMC Mol Biol* **9**:98.
- Gasser PJ, Orchinik M, Raju I, and Lowry CA (2009) Distribution of organic cation transporter 3, a corticosterone-sensitive monoamine transporter, in the rat brain. *J Comp Neurol* **512**:529–555.
- Greengard P (2001) The neurobiology of dopamine signaling. *Biosci Rep* **21**:247–269.
- Gründemann D, Liebich G, Kiefer N, Köster S, and Schömig E (1999) Selective substrates for non-neuronal monoamine transporters. *Mol Pharmacol* **56**:1–10.
- Gründemann D, Schechinger B, Rappold GA, and Schömig E (1998) Molecular identification of the corticosterone-sensitive extraneuronal catecholamine transporter. *Nat Neurosci* **1**:349–351.
- Hayer-Zillgen M, Brüss M, and Bönisch H (2002) Expression and pharmacological profile of the human organic cation transporters hOCT1, hOCT2 and hOCT3. *Br J Pharmacol* **136**:829–836.
- Iversen LL (1971) Role of transmitter uptake mechanisms in synaptic neurotransmission. *Br J Pharmacol* **41**:571–591.
- Kekuda R, Prasad PD, Wu X, Wang H, Fei YJ, Leibach FH, and Ganapathy V (1998) Cloning and functional characterization of a potential-sensitive, polyspecific organic cation transporter (OCT3) most abundantly expressed in placenta. *J Biol Chem* **273**:15971–15979.
- Koepsell H, Lips K, and Volk C (2007) Polyspecific organic cation transporters: structure, function, physiological roles, and biopharmaceutical implications. *Pharm Res* **24**:1227–1251.
- Lynch GS and Ryall JG (2008) Role of β -adrenoceptor signaling in skeletal muscle: implications for muscle wasting and disease. *Physiol Rev* **88**:729–767.
- Mathews TA, Fedele DE, Coppelli FM, Avila AM, Murphy DL, and Andrews AM (2004) Gene dose-dependent alterations in extraneuronal serotonin but not dopamine in mice with reduced serotonin transporter expression. *J Neurosci Methods* **140**:169–181.
- Nourian Z, Mulvany MJ, Nielsen KB, Pickering DS, and Kristensen T (2008) The antagonistic effect of antipsychotic drugs on a HEK293 cell line stably expressing human α 1-adrenoceptors. *Eur J Pharmacol* **596**:32–40.
- Romanowski T, Sikorska K, and Bielawski KP (2008) GUS and PMM1 as suitable reference genes for gene expression analysis in the liver tissue of patients with chronic hepatitis. *Med Sci Monit* **14**:BR147–BR152.
- Schildkraut JJ and Mooney JJ (2004) Toward a rapidly acting antidepressant: the normetanephrine and extraneuronal monoamine transporter (uptake 2) hypothesis. *Am J Psychiatry* **161**:909–911.
- Slitt AL, Cherrington NJ, Hartley DP, Leazer TM, and Klaassen CD (2002) Tissue distribution and renal developmental changes in rat organic cation transporter mRNA levels. *Drug Metab Dispos* **30**:212–219.
- Torres GE, Gainetdinov RR, and Caron MG (2003) Plasma membrane monoamine transporters: structure, regulation and function. *Nat Rev Neurosci* **4**:13–25.
- Ungar A and Phillips JH (1983) Regulation of the adrenal medulla. *Physiol Rev* **63**:787–843.
- Vialou V, Balasse L, Dumas S, Giros B, and Gautron S (2007) Neurochemical characterization of pathways expressing plasma membrane monoamine transporter in the rat brain. *Neuroscience* **144**:616–622.
- Weichert D, Gobom J, Klopffleisch S, Häslar R, Gustavsson N, Billmann S, Lehrach H, Seeger D, Schreiber S, and Rosenstiel P (2006) Analysis of NOD2-mediated proteome response to muramyl dipeptide in HEK293 cells. *J Biol Chem* **281**:2380–2389.
- Wu X, Huang W, Ganapathy ME, Wang H, Kekuda R, Conway SJ, Leibach FH, and Ganapathy V (2000) Structure, function, and regional distribution of the organic cation transporter OCT3 in the kidney. *Am J Physiol Renal Physiol* **279**:F449–F458.
- Wu X, Kekuda R, Huang W, Fei YJ, Leibach FH, Chen J, Conway SJ, and Ganapathy V (1998) Identity of the organic cation transporter OCT3 as the extraneuronal monoamine transporter (uptake2) and evidence for the expression of the transporter in the brain. *J Biol Chem* **273**:32776–32786.
- Zhou M, Engel K, and Wang J (2007) Evidence for significant contribution of a newly identified monoamine transporter (PMAT) to serotonin uptake in the human brain. *Biochem Pharmacol* **73**:147–154.
- Zhu CB, Blakely RD, and Hewlett WA (2006) The proinflammatory cytokines interleukin-1 β and tumor necrosis factor- α activate serotonin transporters. *Neuropsychopharmacology* **31**:2121–2131.

Address correspondence to: Dr. Joanne Wang, Department of Pharmaceutics, University of Washington, H272J Health Science Bldg, Seattle, WA 98195. E-mail: jowang@u.washington.edu
